A1506

Development of metal foam supported SOFCs

Feng Han[1], Robert Semerad[2] and Rémi Costa[1]

[1]German Aerospace Center
Institute of Engineering Thermodynamics
Pfaffenwaldring 38-40
D-70569 Stuttgart / Germany
Tel.: +49-711-6862-8047
Fax: +49-711-6862-1442
feng.han@dlr.de

[2]Ceraco Ceramic Coating GmbH
Rote-Kreuz-Str. 8
D-85737 Ismaning / Germany

Abstract

A metal foam supported solid oxide fuel cell (SOFC) with yttria-stabilized zirconia (YSZ) and gadolinium doped ceria (GDC) bi-layer electrolyte is proposed. The prepared cells are supported by NiCrAl metal foam, which has been impregnated with La-substituted $SrTiO_3$ (LST) as electrical conductive material. An LST-GDC anode functional layer was tape cast into green tape and then laminated onto the metal foam support. The measured thickness of the anode functional layer is approximately 20 µm after calcination at 1000 ^{o}C. Gas-tight YSZ electrolyte layers were deposited by vacuum plasma spray (VPS). Alternatively, porous YSZ layers were dip-coated with a fine suspension containing YSZ nanoparticles in order to obtain thin-film electrolytes. Successively, a gas-tight GDC electrolyte was deposited by EB-PVD method. The thickness of the gas-tight VPS YSZ electrolyte and the thin film YSZ-GDC bi-layer electrolyte was approximately 100 µm and 3 µm, respectively. The pore size distribution of NiCrAl foam supported substrates was characterized by mercury porosimetry analysis, the microstructure was demonstrated with SEM and the gas-tightness of the half cells was evaluated.

1. Introduction

Solid oxide fuel cells (SOFCs) are regarded as high efficient energy conversion devices, which directly generate electrical power from a variety of chemical fuels. Metal supported cells (MSCs) apply porous metal substrates to replace the conventional ceramic or cermet supports in SOFC design. The potential advantages of MSCs include cost-effective material options, improved mechanical robustness, thermal shock resistance and fast start-up capability [1, 2]. These features make MSCs especially attractive for mobile applications such as auxiliary power units (APUs). As interconnect materials for SOFCs, Cr-containing alloys with good oxidation resistance are suitable for application in intermediate temperatures range of 600–800 ^{o}C [2–7]. However, processing issues remain as challenges for the fabrication of MSCs. In the case of ceramic or cermet supported cells, conventional sintering process at over 1200 ^{o}C are normally accompanied with shrinkage of the components, which favors the densification of electrolytes. On the contrary, metal supported cells (MSC) hardly shrink and are often not chemically or mechanically stable at the high temperature during the electrolyte sintering process. It is necessary to avoid exposing the MSCs to excessive high-temperature over 1200 ^{o}C during the cell manufacturing process. Physical deposition methods are extremely attractive for the low temperature (400-800 ^{o}C) fabrication of electrolyte on metal supports [3, 5, 7].

The state-of-the-art MSCs mainly apply Ni/YSZ cermet as anode due to the excellent catalytic activities and electrical conductivity. However, unsolved problems, including Ni agglomeration, coking, sulfur poisoning and redox cycling instability, remain obstacles for the commercialization of SOFCs based on Ni/YSZ cermet anodes [8-12]. $SrTiO_3$-based materials are considered as alternative to overcome the limitations of Ni/YSZ cermet. Lanthanum or yttrium-substituted $SrTiO_3$ demonstrates properties of high electrical conductivity after thermally treated in reducing atmosphere, similar thermal expansion coefficient as that of YSZ and excellent dimensional stability upon redox cycling [13-17]. However, porous lanthanum or yttrium-substituted $SrTiO_3$ substrates with typical thickness of less 500 µm cannot provide reliable mechanical stability. Porous metal substrates may be applied for supporting or strengthen the $SrTiO_3$-based anode materials.

In this work, a novel cell design with NiCrAl metal foam as structural substrate support, impregnated LST ceramic as anode material and a gas-tight VPS YSZ electrolyte or a thin film YSZ-GDC bi-layer electrolyte are demonstrated and investigated.

2. Experiments

2.1 $La_{0.1}Sr_{0.9}TiO_3$ (LST) powder
The as-received LST powder (CerPoTech, Norway) was measured with a specific surface area of 9.5 m^2/g. The LST powder was coarsened by firing the LST powder at 1200 ^{o}C with heating rate of 180 K/h and dwelling time for 5 h.

2.2. Slurry preparation
2.2.1 Slurry for impregnation
The powders were milled in methyl-ethyl-ketone (MEK)/ethanol solvent for 6 h to form suspensions. Polyvinyl butyral (PVB, Sigma-Aldrich, Germany) and polyethylene glycol

(PEG, Sigma-Aldrich, Germany) were added and mixed into to the suspensions. Homogeneous slurries with LST powder were obtained after another 6 h milling process.

2.2.2 Slurry for anode functional layer deposition
LST powder (CerPoTech, Norway) and $Gd_{0.2}Ce_{0.8}O_2$ (GDC) powder (Treibach AG, Austria) are well mixed and milled in MEK/ethanol solvent for 24 h to obtain a suspension. PVB (Sigma-Aldrich, Germany) and PEG (Sigma-Aldrich, Germany) were added and mixed into to the suspension. The homogeneous slurry was obtained after another 6 h milling process.

2.3 Substrate preparation
NiCrAl foam (Alantum GmbH, Germany) was cut into round substrates with diameter of 48 mm. The substrates were impregnated with LST slurry and dried at 75 ^{o}C for 30 min. Then the substrates were uni-axially pressed to increase the LST powder packing density and reduce the substrate thickness.

2.4 Anode Layer
The LST-GDC slurry was cast with a doctor blade into a green tape with a thickness of 35 µm. The green tape was laminated onto the substrates under a uni-axial pressure. The substrate and the anode layer were co-fired at 1000 ^{o}C with a heating rate of 3 K/min and dwelling time of 1 to 3 hours.

2.5 YSZ layer
2.5.1
Vacuum Plasma Spray (VPS) was applied to produce the thick YSZ layer, the experimental details were reported elsewhere in literature [5].

2.5.2
Thin-film YSZ layer was deposited by dip-coating of aqueous YSZ nano-suspension. The experimental details were reported elsewhere in literature [18].

2.6 Deposition of the thin film GDC Layer
$Gd_{0.2}Ce_{0.8}O_2$ (GDC) layers were fabricated by electron beam physical vapor deposition (EB-PVD) method.

2.7 Characterization
Zeiss ULTRA PLUS SEM (Carl Zeiss AG, Germany) with an X-Flash Detector 5010 (Bruker, Germany) were used for SEM and elemental mapping investigation of the samples. The gas-tightness of the electrolyte was characterized by an air leakage testing module (DLR, Germany). Porosity characterization was carried out on a Pascal Mercury Porosimeters 140 + 240 (Thermo Scientific, Germany). BET measurement was done on a Sorptomatic 1990 (Thermo Scientific, Germany).

3. Results

It is observed in Figure 1 (a) that the NiCrAl alloy foam has an open pore size of about 450 µm. In order support the anode and electrolyte, the pore size of the substrates was reduced to submicron range through the impregnation of LST ceramic into the metal foam and a calcination at 1000 ^{o}C, as shown in Figure 1 (b). The NiCrAl metal foam as the structural framework ensured the mechanical strength of the substrates. The pore size of

the LST-GDC anode is further reduced to less than 100 nm, as seen in Figure 1 (c), which is suitable to support the dip-coated YSZ layer. Figure 1 (d) shows that the dip-coated YSZ layer is consisted of fine nanoparticles.

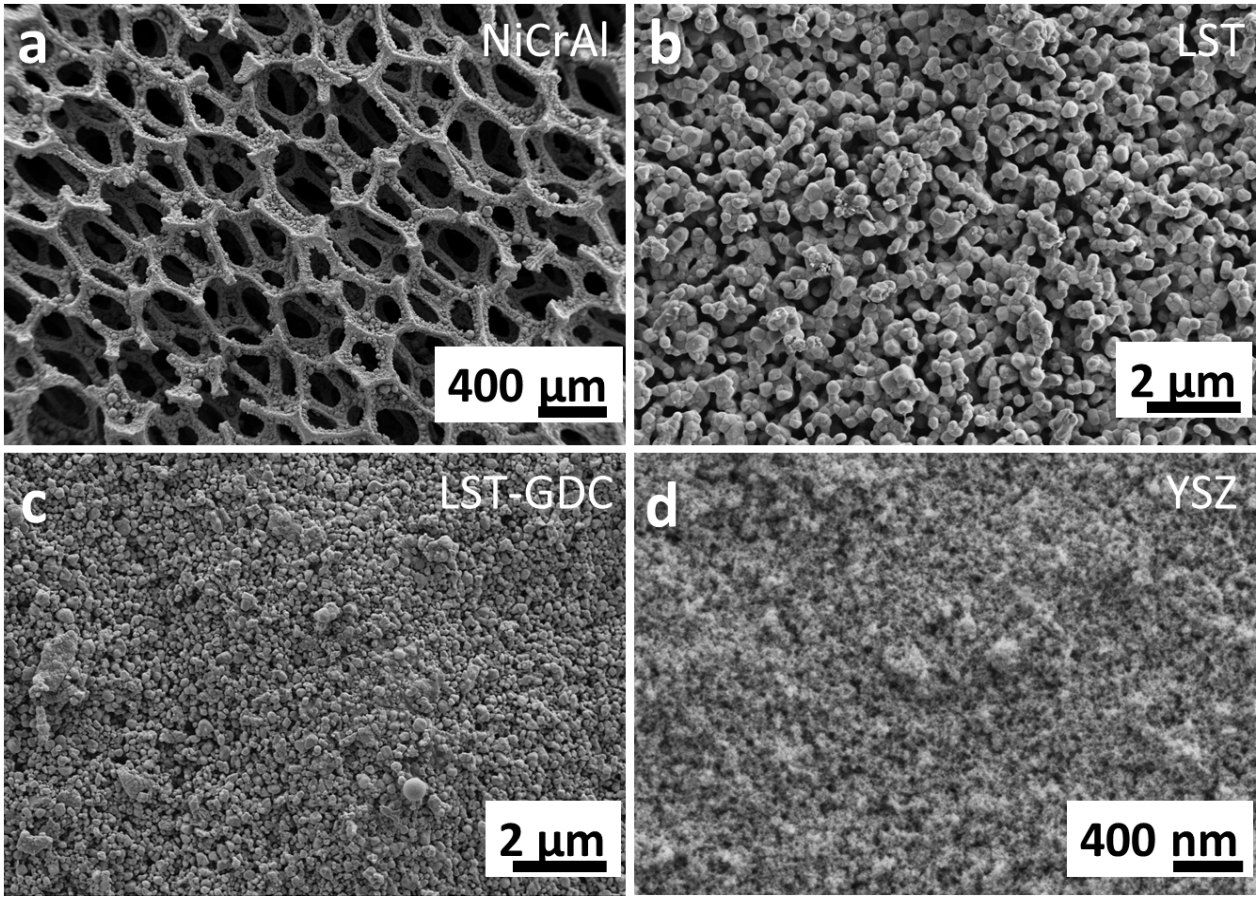

Figure 1 Top view SEM: (a) NiCrAl foam, (b) NiCrAl foam with impregnated LST, (c) LST-GDC anode functional layer, (d) dip-coated YSZ layer

The pore size of the substrates has been adjusted by processing parameters, such as particles size of LST powders and the thermal treatment conditions. In general, higher calcination temperature can significantly reduce the specific surface area of the LST powders, enlarge the particle size and pore size. According to BET measurements, the specific surface area values of LST powder fired at 1100 ^{o}C for 6 h and 1200 ^{o}C for 5 h are 9.5 m^2/g and 3.0 m^2/g, respectively. It is observed in Figure 2 (a) that the modal pore diameter of the substrate impregnated with fine LST powder and fired at 1000 ^{o}C for 1 h is 79 nm. Fired at 1000 ^{o}C for 3 h, the modal pore diameter of the substrate was enlarged to 164 nm and the cumulative pore volume slightly reduced from 83.8 mm^3/g to 75.8 mm^3/g, as shown Figure 2 (b). In the other case, the LST powder was first coarsened at 1200 ^{o}C for 5 h before the impregnation into the NiCrAl foam. It can be seen in Figure 2 (c) that the modal pore diameter and the cumulative pore volume of the substrate impregnated with coarsened LST powder and fired at 1000 ^{o}C for 1 h was 216.2 nm and 94.1 mm^3/g, respectively. By prolonging the dwelling time to 3 h, the modal pore size was enlarged to 355 nm and the cumulative pore volume was measured as 178 mm^3/g, as shown in Figure 2 (d).

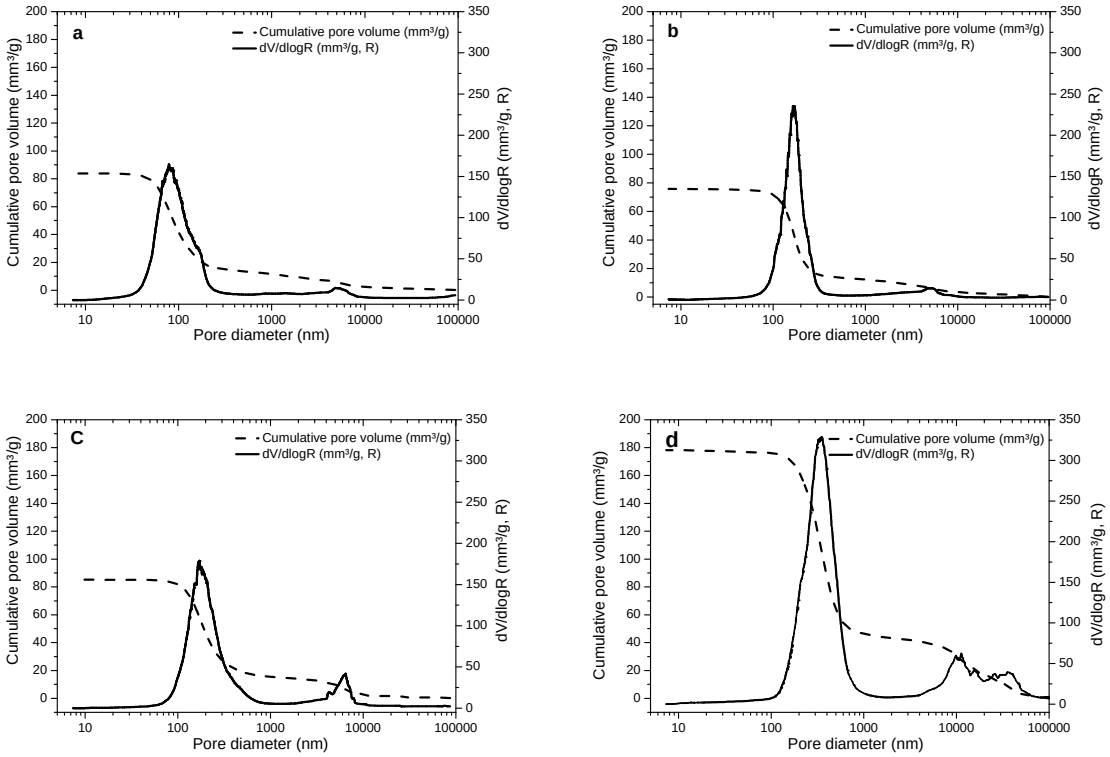

Figure 2 Pore size distribution of calcined NiCrAl alloy substrates with impregnated LST: (a) 1000 °C 1h with fine LST, (b) 1000 °C 3 h with fine LST, (c) 1000 °C 1h with coarsened LST, (d) 1000 °C 3 h with coarsened LST

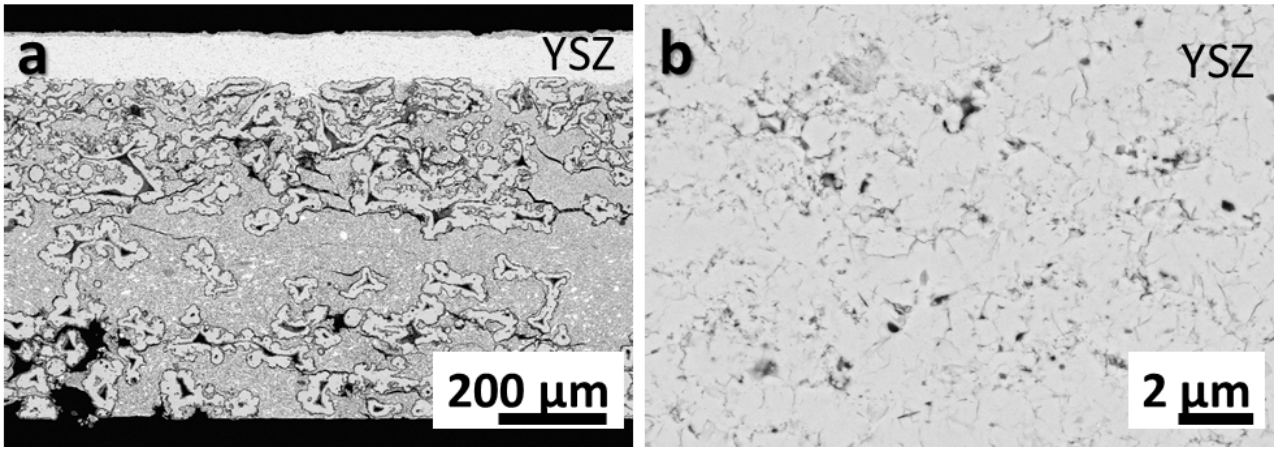

Figure 3 SEM: (a) cross section of a half cell with VPS YSZ electrolyte, (b) surface of the VPS YSZ electrolyte

As demonstrated in Figure 3 (a), YSZ electrolyte prepared on the metal foam support with VPS technology has a thickness about 100 µm in order to ensure the necessary gas-tightness level, corresponding to an air leakage rate below $5x10^{-3}$ (hPa dm^3)/(s cm^2). It is also observed in the SEM cross section that the laminated LST-GDC anode functional layer has been completely removed by VPS process because it cannot withstand the strong mechanical impact from the molten YSZ splat with high velocity. It is observed in Figure 3 (b) that the surface of the YSZ electrolyte is rough and with plenty of defects. An excellent performance with high power density cannot be expected on cells with such thick VPS YSZ electrolyte.

Aiming to reduce the electrolyte thickness, thin film YSZ electrolyte was deposited by dip-coating method. It is observed in Figure 5 (a) and (c) that the YSZ layer and an EB-PVD GDC layer has been homogenously deposited on top of the LST-GDC anode layer. The thickness of the calcined LST-GDC anode layer is about 20 µm. The total thickness of the crack-free YSZ and GDC double layer is approximately 3 µm. The top view of fine structured GDC layer is shown in Figure 5 (b), reveals that the GDC layer is dense and the average grain size is below 200 nm. The elemental mapping for the SEM in Figure 4 (c) is shown in Figure 4 (d), indicating that no obvious elemental interdiffusion between the YSZ and GDC phases has happened at the LST-GDC/YSZ/GDC interfaces. With the homogenous YSZ layer and the dense GDC layer, the half cells realized excellent gas-tightness with air leakage rate values as low as $2x10^{-3}$ (hPa dm^3)/(s cm^2) despite the extremely thin electrolyte.

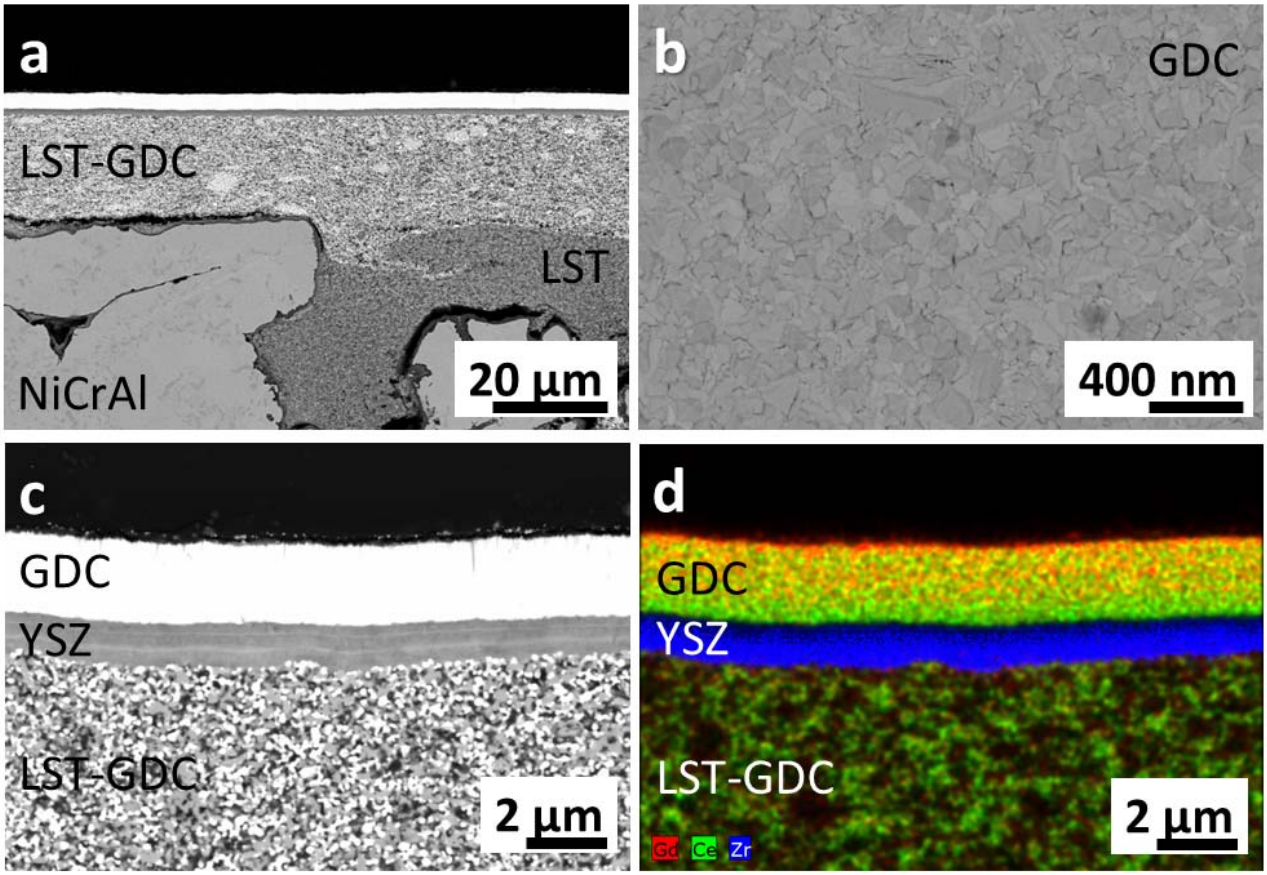

Figure 4 SEM of half cells with dip-coated YSZ layer and EB-PVD GDC layer: (a) overview cross section, (b) top view of GDC layer, (c) cross section at LST-GDC/YSZ/GDC interfaces, (d) elemental mapping at LST-GDC/YSZ/GDC interfaces

4. Conclusion

Half cells have been fabricated on substrates consisting of NiCrAl alloy foam as structural support and impregnated LST ceramic as anode material. Gas-tight YSZ electrolyte of 100 µm thick was deposited by VPS technology. Thin-film YSZ-GDC bi-layer electrolytes were made of dip-coated 1 µm thick YSZ layers and 2 µm thick EB-PVD GDC layers. Despite the extremely thin electrolyte, the leakage rate of the half cells with thin-film YSZ-GDC bi-layers has been measured as low as $2x10^{-3}$ (hPa dm^3)/(s cm^2), demonstrating an acceptable gas-tightness. The electrochemical tests of the cells will follow in future work.

5. Acknowledgment

The research leading to these results has received funding from the European Union's Seventh Framework Programme (FP7/2007-2013) for the Fuel Cells and Hydrogen Joint Technology Initiative under grant agreement No. 303429 (Project EVOLVE). The authors also thank Ina Plock, Gudrun Steinhilber, Davide Vattuone and Tang Rui for all experimental supports and helpful discussions.

References

[1] M. C. Tucker, G. Y. Lau, C. P. Jacobson, L. C. DeJonghe, S. J. Visco, Performance of Metal-supported SOFCs with Infiltrated Electrodes, Journal of Power Sources, 171, (2007) 477-482.

[2] M. C. Tucker, Progress in Metal-supported Solid Oxide Fuel Cells: A review, Journal of Power Sources, 195, (2010) 4570-4582.

[3] R. Vaßen, D. Hathiramani, J. Mertens, V.A.C. Haanappel, I.C. Vinke, Manufacturing of High Performance Solid Oxide Fuel Cells (SOFCs) with Atmospheric Plasma Spraying (APS), Surface & Coatings Technology, 202, (2007) 499–508.

[4] T. Franco, R. Henne, M. Lang, G. Schiller, P. Szabo, F. Meyer, L. Otterpohl, Novel Metallic Substrate Materials for Plasma Sprayed Thin-Film SOFCs, 5th European Solid Oxide Fuel Cell Forum, Luzern, Schweiz, July 2002.

[5] M. Lang, T. Franco, G. Schiller, N. Wagner, Electrochemical Characterization of Vacuum Plasma Sprayed Thin-film Solid Oxide Fuel Cells (SOFC) for Reduced Operating Temperatures, Journal of Applied Electrochemistry, 32, (2002) 871-874.

[6] M. Lang, P. Szabo, Z. Ilhan, S. Cinque,T. Franco, G. Schiller, Development of Solid Oxide Fuel Cells and Short Stacks for Mobile Application, Journal of Fuel Cell Science and Technology, 4, (2007) 384-391.

[7] M. Haydn, K. Ortner, T. Franco, S. Uhlenbruck, N. H. Menzler, D. Stöver, G. Bräuer, A. Venskutonis, L. S. Sigl, H. P. Buchkremer, R. Vaßen, Multi-layer Thin-film Electrolytes for Metal Supported Solid Oxide Fuel Cells, Journal of Power Sources, 256, (2014) 52-60.

[8] H. Tu, U. Stimming, Advances, Aging Mechanisms and Lifetime in Solid Oxide Fuel Cells, Journal of Power Sources 127, (2004) 284-293.

[9] S. McIntosh, R.J. Gorte, Direct Hydrocarbon Solid Oxide Fuel Cells, Chemical Reviews, 104, (2004) 4845-4866.

[10] S. Zha, Z. Cheng, M. Liu, Sulfur Poisoning and Regeneration of Ni- Based Anodes in Solid Oxide Fuel Cells, Journal of The Electrochemical Society, 154, (2007) B201-206.

[11] D. Sarantaridis, A. Atkinson, Redox Cycling of Ni-Based Solid Oxide Fuel Cell Anodes: A Review, Fuel Cells, 7, (2007) 246-258.

[12] A. Faes, A. Nakajo, A. Hessler-Wyser, D. Dubois, A. Brisse, S. Modena, J. Van herle, Redox Study of Anode-supported Solid Oxide Fuel Cell, Journal of Power Sources, 193, (2009) 55-64.

[13] S. Q. Hui, A. Petric, Electrical Properties of Yttrium-Doped Strontium Titanate under Reducing Conditions, Journal of The Electrochemical Society, 149 (2002) J1-J10.

[14] O. A. Marina, N. L. Canfield, J. W. Stevenson, Thermal, Electrical, and Electrocatalytical Properties of Lanthanum-doped Strontium Titanate, Solid State Ionics, 149, (2002) 21-28.

[15] Q. X. Fu, F. Tietz, D. Sebold, S. W. Tao, J. T. S. Irvine, An Efficient Ceramic-based Anode for Solid Oxide Fuel Cells, Journal of Power Sources, 171, (2007) 663-669.

[16] Q. Ma, F. Tietz, A. Leonide, E. Ivers-Tiffée, Anode-supported Planar SOFC with High Performance and Redox Stability, Electrochemistry Communications, 12, (2010) 1326-1328.

[17] M. R. Pillai, I. Kim, D. M. Bierschenk, S. A. Barnett, Fuel-flexible Operation of a Solid Oxide Fuel Cell with $Sr_{0.8}La_{0.2}TiO_3$ Support, Journal of Power Sources, 185, (2008) 1086-1093.

[18] T. Van Gestel, F. Han, D. Sebold, H. P. Buchkremer, D. Stöver, Nano-structured Solid Oxide Fuel Cell Design with Superior Power Output at High and Intermediate Operation Temperatures, Microsystem Technologies, 17-2, (2011) 233-242.